J Mater Sci: Mater Electron (2017) 28:2462–2470
DOI 10.1007/s10854-016-5819-0

Synthesis and luminescent behavior of UV induced Dy^{3+} activated $LaAlO_3$

D. Singh[1] · J. Kaur[1] · N. S. Suryanarayana[1] · R. Shrivastava[2] · V. Dubey[3]

Received: 2 July 2016 / Accepted: 3 October 2016 / Published online: 5 November 2016

Abstract Dy^{3+} doped Lanthanum Aluminate phosphors are prepared for different concentrations of dopant and the luminescent properties of the phosphor are studied. High temperature modified solid-state reaction method is used for the synthesis. XRD analysis confirms the formation of $LaAlO_3$:Dy^{3+} phosphor. Average crystallite size calculated is 40.085 nm.Thermoluminescence study of UV induced $LaAlO_3$:Dy^{3+} phosphor is discussed in this paper. Thermoluminescence glow peak is recorded for different UV exposure time and for different concentrations of dopant. Kinetic parameters such as shape factor, activation energy, order of kinetics are calculated by using computerized glow curve deconvolution technique. Activation energy varies from 0.63 to 0.72 eV. The TL glow curve intensity varies nearly linear with increasing UV dose. Photoluminescence (PL) emission spectra are recorded for different concentrations of dopant. Highest intensity of PL emission was obtained for 1.5 mol% of Dy^{3+} doped $LaAlO_3$ phosphor. The excitation spectra of Dy^{3+} doped $LaAlO_3$ phosphor monitored at 550 nm shows broad band around 260 nm and a sharp peak at 394 nm. Peaks with lower intensity are obtained at 320 nm, 363 nm and 384 nm. In the Pl emission spectra, peak at 554 nm (yellow greenish) has highest intensity. Peaks with less intensity are obtained at 466 nm (blue), 645 nm (orange red) and 740 nm (brownish red). Pl intensity varies linearly with increasing concentration of dopant. CIE chromaticity coordinates are calculated for $LaAlO_3$:Dy^{3+} (1.5 mol%), $x = 0.3586$ and $y = 0.5421$ which corresponds to yellow–greenish region. The prepared phosphor may find application in dosimetry and optical devices.

✉ D. Singh
deepti27.singh@gmail.com

[1] Department of Physics, Govt. V.Y.T. P.G. Auto. College, Durg, C.G., India

[2] Department of Physics, ICFAI University, Kumhari, Raipur, C.G., India

[3] Department of Physics, B.I.T., Raipur, C.G., India

1 Introduction

$LaAlO_3$ is reported to be a good host material due to its interesting properties such as wide band-gap (~5.6 eV), significantly low phonon energy (146–159 cm^{-1}), good transparency over visible light range and good thermal and chemical stability [1–6]. $LaAlO_3$ crystals belong to perovskite, group which follows the general formula ABO_3. $LaAlO_3$ has wide range of applications owing to its fascinating physical and chemical properties. Dy^{3+} ($^4f_9$) is one of the most efficient rare-earth ions having applications in optical devices because of its abundant emission colors according to their 4f-4f transitions. It is well known from the literature data that the active Dy^{3+} ion possesses two strong luminescence bands in the visible range including blue ($^4F_{9/2} \rightarrow {}^6H_{15/2}$,486 nm) and yellow ($^4F_{9/2} \rightarrow {}^6H_{13/2}$, 576 nm) which are easily affected by the external crystal field. The analysis of luminescence from $^4F_{9/2}$ level of Dy^{3+} is very appealing as it covers the visible and near infra-red regions [7].

In the present work, Dy^{3+} doped $LaAlO_3$ phosphor is synthesized and its luminescent properties are studied. The effects of Dy^{3+} concentration on the thermoluminescence glow curve intensity and photoluminescence emission spectra are also discussed. Average crystallite size of the prepared phosphor is also calculated.

2 Experimental

High temperature modified solid-state reaction method was used for the synthesis of $LaAlO_3:Dy^{3+}$ phosphor. Starting materials used were La_2O_3, Al_2O_3, $Dy_2O_3$and H_3BO_3 (as flux). Stoichiometric ratios of the raw materials were taken and thoroughly grinded in mortar pestle for about 45 min for the proper mixing. The finely grinded homogeneous powder was then transferred to an alumina crucible and placed inside the muffle furnace for calcination at 1000 °C and then sintered at 1250 °C for 2 h. Every heat treatment was followed by intermediate grinding. The resulting sample was allowed to cool down at room temperature and then grinded for few minutes to obtain finely powdered phosphor [8].

The synthesis route is very easy and does not require expensive as well as sophisticated equipments. Such a high temperature leads to the formation and crystallization of phosphor materials. The most important advantage of solid-state reaction method is that the final product in solid form is structurally pure with desired properties depending on the final sintering temperatures [9]. Until now, this technique has been employed to produce a variety of materials such as oxides, borates, silicates and carbonates.

The resultant product is the phosphor which occupies the entire volume of the reaction vessel. The energy released from exothermic reaction between the starting materials and fuel can quickly heat the system to high temperatures without an external heat source. Synthesized phosphors powders are generally more consistent, have fewer impurities, and have higher surface areas than powders prepared by conventional solid state methods [10]. All the measurements were performed at room temperature. In this process the powders produced from solid-state reaction method is very fine and the cross contamination is very less. This method is environment friendly as no toxic or unwanted waste is produced after the solid-state reaction is complete. This method is also very convenient for large scale production on industrial scale [11, 12].

For XRD analysis of the sample Bruker D8 Advance X-ray Diffractometer was used. The wavelength of X-rays used here is 0.154(Cu K-alpha). A sealed tube was used for producing X-rays. The X-rays were detected using a fast counting detector based on Silicon strip technology. The Photoluminescence excitation and emission spectra were recorded at room temperature using Shimadzu RF-5301 PC spectrofluorophotometer. A Xenon lamp was used as the source of excitation. TLD reader 11009 supplied by Nucleonix Sys. Pvt. Ltd. Hyderabad was used to record thermally stimulated glow curves. Heating rate used for recording TL glow curve was 6.7 °C/s. Different glow curves were recorded for different concentrations of dopant. Also the effect of variation in the UV exposure ($\sim$365 nm) time on the glow curve of the samples were studied.

3 Result and discussion

3.1 XRD analysis of $LaAlO_3:Dy^{3+}$

For obtaining the lattice parameters of the sample the powder diffraction pattern was analyzed by Rietveld fitting method [13]. Lattice parameters were refined until the observed and calculated XRD spectra were fairly in good agreement. The pattern is characterized by few prominent peaks found at different glancing angles.

The crystallite size was computed from the full width half maxima (FWHM) of every peak using the Scherer's formula [14].

The Scherer's formula is given by:

$$D = \frac{0.9\lambda}{\beta \cos\theta}$$

where, D = crystallite size; λ = wavelength of X-rays β = FWHM θ = diffraction angle

Calculated crystallite size for different angle of glancing is shown in Table 1. The average crystallite size is 40.085 nm.

Figure 1 represents the XRD pattern of Lanthanum Aluminate doped with Dy^{3+} ions. Celref v.3 software is used for indexing and refinement parameters. It shows trigonal structure on hexagonal axis with space group R-3c (167). The refined values of lattice parameters of Dy doped Lanthanum aluminate are: a = 5.3864; c = 13.1907, which is illustrated in Table 2.

Table 1 Structural parameters of prepared phosphor ($LaAlO_3:Dy^{3+}$)

2θ	FWHM(β)	d spacing	D (crystallite size) nm
23.422	0.273	3.795	31.05
32.677	0.091	2.738	95.06
33.269	0.286	2.691	30.29
41.044	0.286	2.197	30.99
47.762	0.299	1.903	30.36
48.411	0.403	1.879	22.58
53.785	0.299	1.703	31.13
55.035	0.312	1.667	30.00
59.396	0.364	1.555	26.25
69.775	0.338	1.347	29.93
74.662	0.234	1.27	44.60
74.780	0.195	1.269	53.57
79.489	0.26	1.205	41.51
79.524	0.169	1.204	63.87

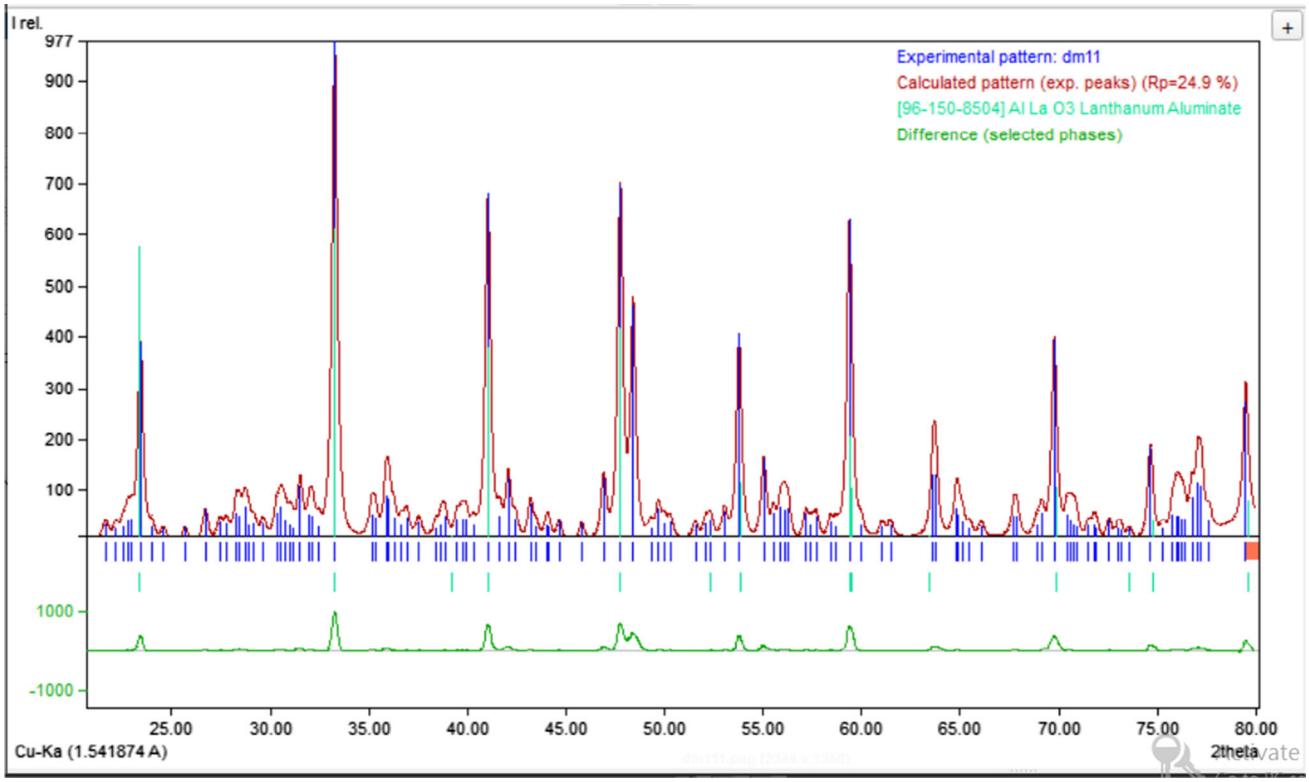

Fig. 1 XRD pattern of Dy^{3+} doped $LaAlO_3$

Table 2 Indexing and lattice parameters of $LaAlO_3$:Dy^{3+}

Zero	Lambda	A	B	C	Alpha	Beta	Gamma	Vol.
Initial values : (Refinement keys on 2nd line)								
0	1.5418	5.3864	5.3864	13.1907	90	90	120	331.4
0	0	1	0	1	0	0	0	
Final values : (Standard errors on 2nd line)								
0	1.5418	5.3952	5.3952	12.9899	90	90	120	327.5
0	0	0.0137	0	0.0044	0	0	0	

H	K	L	2T(Obs)	2T-Zero	2Th(Cal)	Dif
0	1	2	23.422	23.422	23.454	−0.032
1	0	4	33.269	33.269	33.607	−0.338
2	0	2	41.044	41.044	41.0578	−0.0138
0	2	4	47.762	47.762	47.9699	−0.2079
0	2	4	48.411	48.411	47.9699	0.4411
1	2	2	53.785	53.785	53.7923	−0.0073
3	0	0	59.396	59.396	59.3361	0.0599
2	2	0	69.775	69.775	69.7163	0.0587
1	1	9	74.662	74.662	74.5669	0.0951
1	3	4	79.489	79.489	79.6581	−0.1691

4 Thermoluminescence study

4.1 Effect of different UV dose on the intensity of glow peak

Thermoluminescence is the enhancement of the radiative emission of materials by the application of heat which are already being excited electronically. The crystal phosphors that respond to Tl, contain certain traps which are the imperfections or defects in the crystal lattice. The electrons absorb excitation energy and get ejected from the luminescent center. The electrons then get captured in these traps. Trapped electrons absorb the additional thermal energy in order to get released from the traps and recombine with a center and undergo radiative transition [15]. Figure 2a–g shows the TL glow curves of Dy doped Lanthanum aluminate phosphor for 0.1, 0.2, 0.5, 1.0, 1.5, 2.0 and 2.5 mol% concentration of Dy^{3+} with a single prominent peak centered at 175, 202, 191, 183, 199, 196, 196 °C respectively. A weak shoulder peak at higher temperature region is also observed which gets more prominent on increasing the concentration of the dopant and can be seen clearly distinct for 1.0 mol% of Dy^{3+}. For higher concentration of dopant the shoulder peak starts to fade. Highest intensity of the glow curve was obtained for UV exposure of 25 min for 0.1 mol%, 10 min for 0.2 mol%, 15 min for 0.5 mol%, 15 min for 1.0 mol%, 25 min for 1.5 mol%, 25 min for 2.0 mol% and 15 min for 2.5 mol%. With further increase in the UV exposure time of prepared samples the glow curve intensity decreases may be due to destroying of trap centers.

4.2 Calculation of kinetic parameter of the thermoluminescence glow curve using CGCD technique

The computerized glow curve deconvolution (CGCD) analysis has been widely applied since 1980 to resolve a complex thermoluminescent glow curve into individual peak components. Once each component is determined, the trapping parameters, activation energy and frequency factor, can be evaluated [16]. TL glow curve of $LaAlO_3$:Dy^{3+} (1.0 mol%) with UV exposure of 15 min is fitted using CGCD technique (Fig. 3). The figure of merit was around 0.87. Three distinct fitted peaks were found by CGCD technique. Table 3 shows the kinetic parameter such as shape factor, activation energy etc. of the fitted curve. These parameters can be estimated using Chen's set of empirical equations [16–18]. Shape factor ranges around $0.42 \sim 0.44$ i.e., nearly first order kinetic which means nearly one trap formed in the sample and the shoulder peak shows the formation of another trap. The value of activation energy varies from 0.63 to 0.72 eV (Table 3).

4.3 Effect of concentration of Dy^{3+} in the intensity of glow peak curve for constant UV exposure of 20 min

TL glow curves Dy^{3+} doped $LaAlO_3$ phosphors for different concentrations of dopant are shown in Fig. 4. It can be easily observed that change in Dy^{3+} concentration affects the intensity of the glow curve. All the samples were irradiated with UV rays for 20 min and the heating rate used was 6.7 °C/s. Glow curve structure has not changed considerably but some minute deflections in the peak position of the glow curve can be seen which may be due to the presence of Al in the host matrix. TL glow curve of the prepared phosphor shows broad single glow curve with a weak shoulder peak at higher temperature side (277 °C) due to defect centers or luminescent centers formed during irradiation of sample. Low temperature peak is due to formation of lower energy traps where as high temperature peak is due to high energy traps. It is worth noting that the shoulder peak gets prominent as we increase the concentration of Dy^{3+} from 0.1 to 1.0 mol% which on further increasing the concentration of Dy^{3+} starts disappearing.

Highest intensity of glow curve is recorded for 2.0 mol% of dopant in the phosphor. On further increasing the concentration of dopant the intensity of the glow curve decreases may be due to concentration quenching.

4.4 Effect of UV dose on the intensity of TL glow curve

Graph is plotted to study the effect of UV dose on the intensity of TL glow curve (Fig. 5). Glow curve structure does not changes for different UV dose, but the intensity of TL glow curve increases nearly linear with increase in UV dose. Maximum intensity is obtained for UV dose of 25 min. The intensity of glow curve decreases for higher UV dose. Thus, the prepared phosphor may find application in dosimetry.

4.5 Photoluminescence study

The Dy^{3+} ion offers a dense energy level scheme in the infra-red spectral region which results in range of absorption peaks. Because of its dense energy level scheme, multi-phonon relaxation is an issue of concern in this ion. Due to the same reason it offers a large range of possible infrared transitions [19].

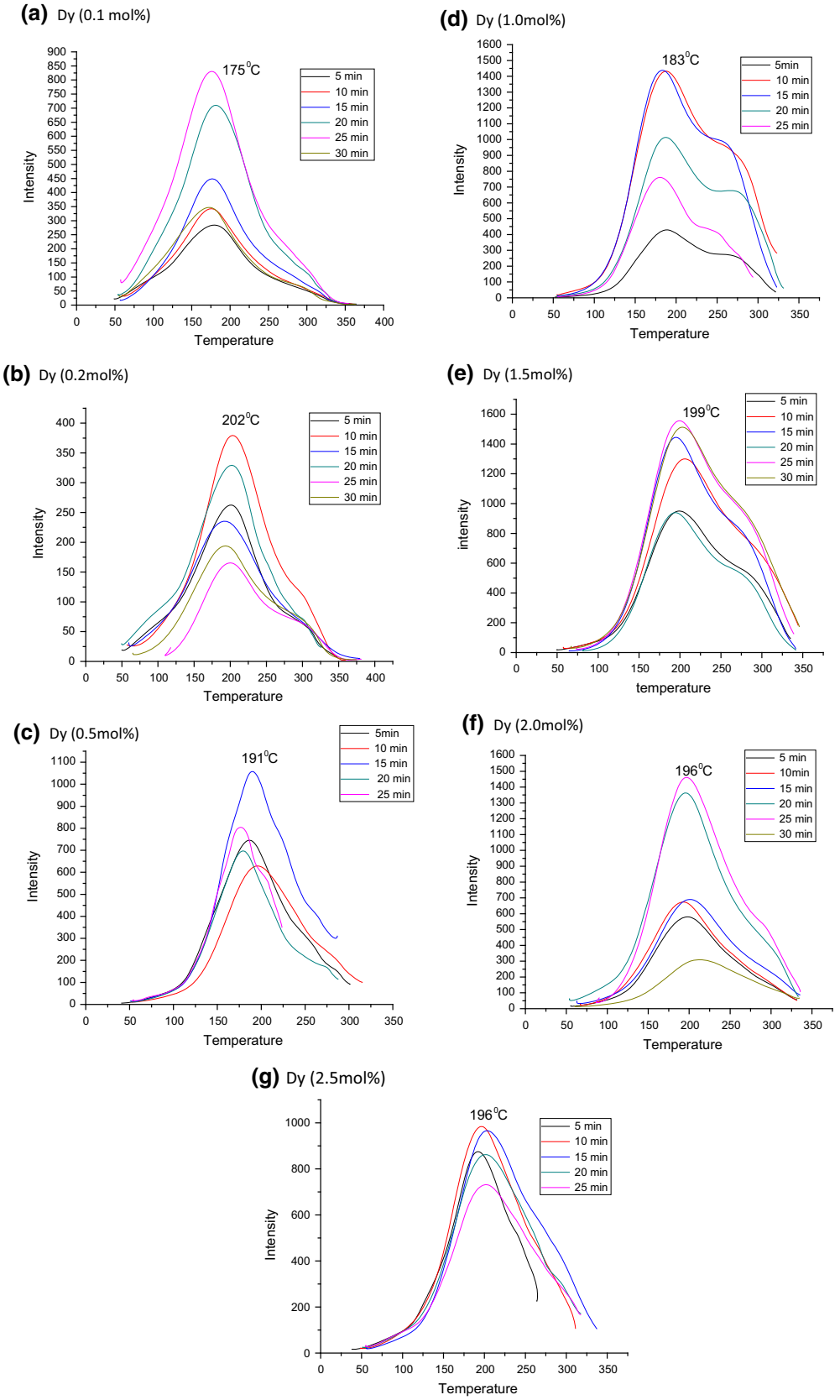

Fig. 2 Thermoluminescence glow curve for different concentration of Dy^{3+} in $LaAlO_3$ phosphor. **a** Dy 0.1 mol%, **b** Dy 0.2 mol%, **c** Dy 0.5 mol%, **d** Dy 1.0 mol%, **e** Dy 1.5 mol%, **f** Dy 2.0 mol%, **g** Dy 2.5 mol%

Figure 6 is the excitation spectra of Dy^{3+} doped $LaAlO_3$ phosphor monitored at 550 nm. A broad band with peak at 268 nm is may be due to Charge transfer (CT) of electrons from the 2p orbital of O^{2-} to the 4f orbital of Dy^{3+}. Peaks are also obtained at 394, 384, and 363 nm which may possibly be due to excitation of electrons from ground state ($^6H_{15/2}$) to higher excited energy states in the $4f^9$ configuration of Dy^{3+}. Table 4 shows the transitions responsible for peaks in the excitation spectra.

Trivalent Dysprosium with $4f^9$ configuration has complicated energy levels and various possible transitions between f levels. The transitions between these f levels are highly selective and of sharp line spectra. It is well known that Dy^{3+} has two intense fluorescence transitions from the $^4F_{9/2}$ level to the $^6H_{15/2}$ and $^6H_{13/2}$ levels [20, 21].

Figure 6 is the excitation spectra of Dy^{3+} doped $LaAlO_3$where peak at 394 nm and a broad peak centered at 268 are of highest intensity. Low intensity peaks are observed at 363 and 384 nm. The emission spectra shows interesting features as Dy^{3+} ion in host lattice shows blue, yellow–greenish and red emission simultaneously (Fig. 7). The emission results from transition from the $^4F_{9/2}$ level to the ground state and other excited energy levels of Dy^{3+}. Most intense peak is found at 554 nm which gives yellow greenish emission. Table 5 below shows the different transition for peaks in the emission spectra [20]. Transition $^4F_{9/2} \rightarrow {}^6H_{15/2}$(blue) is magnetically allowed and is less sensitive to the crystal field and the transition $^4F_{9/2} \rightarrow {}^6H_{13/2}$(yellow greenish) is a forced electric dipole transition with $\Delta J = 2$, which is strongly influenced by

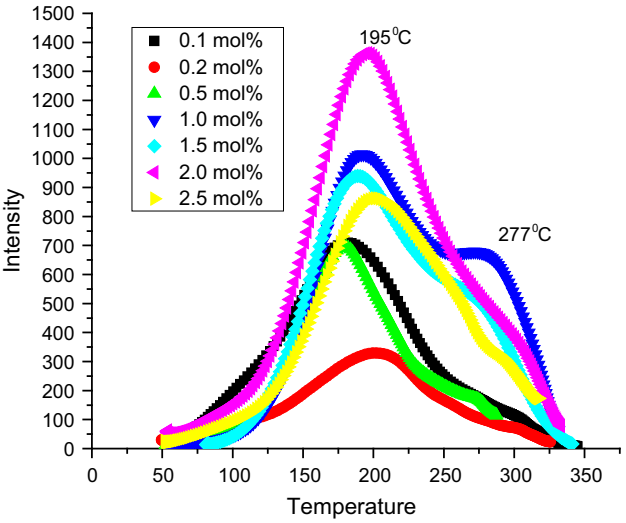

Fig. 4 Variation in the intensity of TL glow for different concentration of dopant in the phosphor

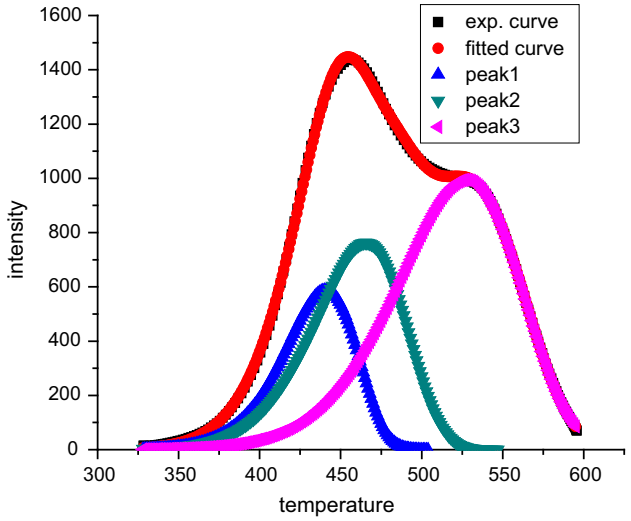

Fig. 3 Thermoluminescence glow curve of Dy^{3+} (1.0 mol%) doped $LaAlO_3$ fitted using CGCD technique

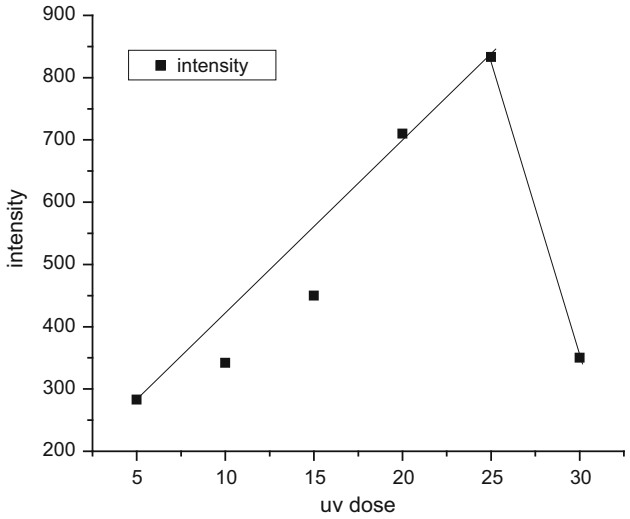

Fig. 5 UV dose Vs TL glow curve intensity for $LaAlO_3$:Dy^{3+} (0.1 mol%) phosphor

Table 3 Calculation of kinetic parameter of CGCD fitted curve

Peaks	T_1	T_m	T_2	τ	δ	ω	$\mu = \delta/\omega$ shape factor	E (eV) Activation energy	S (s^{-1}) frequency factor
Peak 1	409	440	462	31	22	53	0.42	0.7165	1.6×10^8
Peak 2	428	465	493	37	28	65	0.43	0.6717	1.9×10^7
Peak 3	476	526	566	50	40	90	0.44	0.6325	1.2×10^6

host lattice of Dy^{3+} ions. This transition is allowed only at low symmetries with no inversion center and its intensity is strongly influenced by the crystal-field environment.

Photoluminescence emission was recorded for different concentrations of dopant in $LaAlO_3$. Highest intensity was observed for 1.5 mol% Dy^{3+} doped $LaAlO_3$. With further increase in concentration the intensity decreases due to concentration quenching. Cross-relaxation process occurs for ionic pairs and as the concentration of dopant increases more dysprosium pairs are formed. More ions transfer their energy non-radiatively through cross-relaxation processes leading to concentration quenching (Fig. 7).

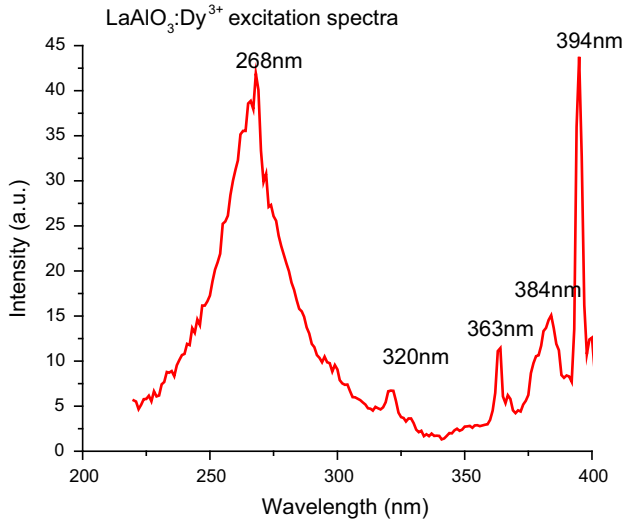

Fig. 6 Excitation spectra of Dy^{3+} doped $LaAlO_3$

Table 4 Transitions in excitation spectra of Dy^{3+} doped $LaAlO_3$

Peaks	Wavelength	Transition
1.	Broad band centered at 268 nm	Due to charge transfer process
2.	320 nm	$^6H_{15/2} \rightarrow {}^6P_{3/2}$
3.	363 nm	$^6H_{15/2} \rightarrow {}^6P_{5/2}$
4.	384 nm	$^6H_{15/2} \rightarrow {}^4K_{17/2}$
5.	394 nm	$^6H_{15/2} \rightarrow {}^4G_{11/2}$

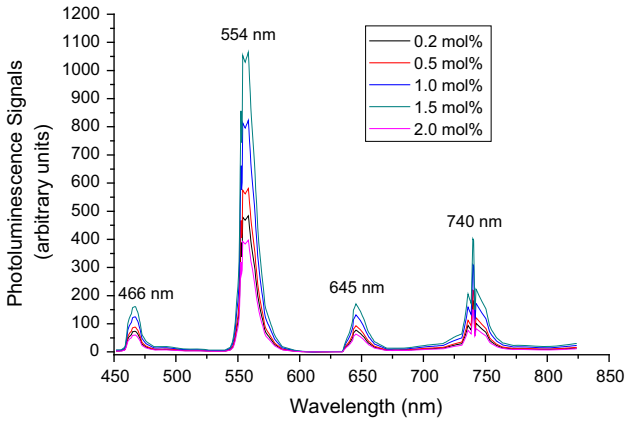

Fig. 7 Emission spectra of Dy^{3+} doped $LaAlO_3$

Table 5 Transition for different peaks in the PL emission spectra

Peaks	Wavelength	Color	Transition
1.	466 nm	Blue	$^4F_{9/2} \rightarrow {}^6H_{15/2}$
2.	554 nm	Yellow greenish	$^4F_{9/2} \rightarrow {}^6H_{13/2}$
3.	645 nm	Orange red	$^4F_{9/2} \rightarrow {}^6H_{11/2}$
4.	740 nm	Brownish Red	$^4F_{9/2} \rightarrow {}^6F_{11/2} + {}^6H_{9/2}$

4.6 Variation of intensity of PL with concentration of dopant

Figure 8 shows the variation in the intensity of PL spectra for blue light with increasing concentration of dopant (Dy^{3+}) in the host lattice ($LaAlO_3$). As the Dy^{3+} concentration increases from 0.2 to 1.5 mol% the intensity increases linearly and for 2.0 mol% the intensity reduces due to concentration quenching. The main cause for concentration quenching with increase in Dy^{3+} concentration is the increase of the resonant energy transfer from the excited $^4F_{9/2}$ energy state to the $^6H_{15/2}$ ground state of the nearby Dy^{3+} ion and the cross relaxation between the donor (excited Dy^{3+} ion) and acceptor (ground Dy^{3+} ion) [22, 23].

4.7 CIE chromaticity co-ordinate

The Commission International de I'Eclairge (CIE) 1931 [24] has been used to determine the chromaticity coordinates which are one of the important factors for evaluation of performance of the prepared phosphors. The chromaticity coordinates x and y are calculated from the below given expressions.

$$x = \frac{X}{X+Y+Z} \quad y = \frac{Y}{X+Y+Z} \tag{2}$$

where, X, Y and Z are the tristimulus values giving the stimulation for each of the three primary colors, red, green and blue. The CIE color coordinates (x, y) of the Dy^{3+} doped $LaAlO_3$ phosphor have been calculated using the emission spectra data and are found to be $x = 0.3586$ and $y = 0.5421$. The CIE coordinates are located in the yellow greenish region and are depicted in the CIE 1931 chromaticity diagram as shown in Fig. 9.

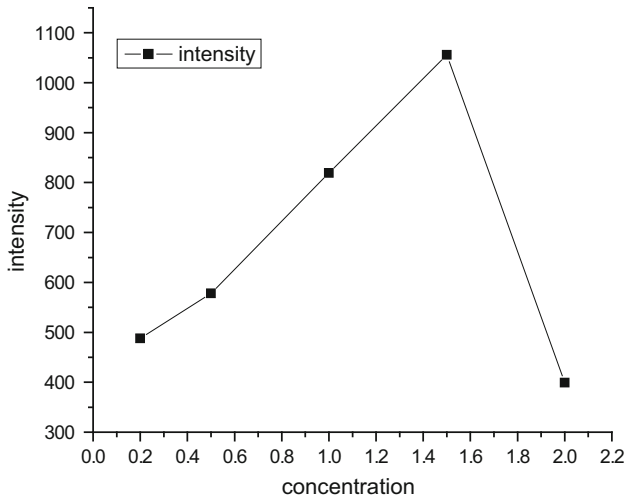

Fig. 8 Variation of PL intensity with Dy^{3+} concentration (in mol%)

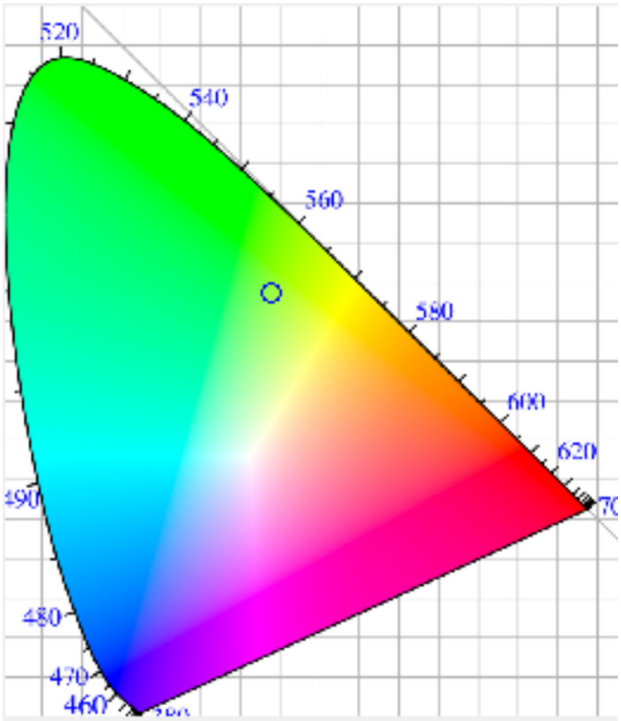

Fig. 9 CIE coordinate of Dy^{3+} doped $LaAlO_3$

5 Conclusion

$LaAlO_3$:Dy^{3+} phosphors for different concentration of Dy^{3+} in $LaAlO_3$ were successfully synthesized using high temperature modified solid-state reaction method.The resultant phosphor is highly pure and there is less chance of cross contamination. This synthesis method is simple and does not require heavy and sophisticated instruments and produces no toxic or harmful chemicals. Average crystallite size was calculated and found to be 40.085 nm. Thermoluminescence glow curves were recorded for all the prepared phosphor with varying UV dose. Dy(1.5 mol%) doped $LaAlO_3$ shows highest intensity of glow curve and is accompanied by a shoulder peak at higher temperature region that fades away for higher concentration of dopant. CGCD method was used for calculating the kinetic parameters. The phosphor shows nearly first order kinetics and the value of activation energy varies from 0.63 to 0.72 eV. TL intensity varies linearly with UV dose which makes it a good candidate to be used in TL detector and dosimetry.PL emission spectra shows emission in red, blue, yellow and green region. The highest intensity is obtained for yellow greenish emission. Highest intensity for PL spectra is seen for 1.5 mol% concentration Dy^{3+}. For higher concentration of dopant the PL intensity decreases due to concentration quenching. CIE chromaticity coordinates are found to be x = 0.3586 and y = 0.5421 which lies in yellow greenish region. The prepared phosphor may find application in display devices.

References

1. M.V. Abrashev, A.P. Litvinchuk, M.N. Iliev, R.L. Meng, V.N. Popov, V.G. Ivanov, R.A. Chakalov, C. Thomsen, Phys. Rev. B **59**, 4146–4153 (1999)
2. J.H. Christopher, J.K. Brendan, C.C. Bryan, J. Phys. Condens. Matter **12**, 349–365 (2000)
3. P. Bouvier, J. Kreisel, J. Phys. Condens. Matter **14**, 3981–3991 (2002)
4. P. Delugas, V. Fiorentinin, A. Filippetti, Phys. Rev. B **71**, 134302 (2005)
5. X.R. Dong, X.Y. Cui, Z.I. Fu, S.H. Zhou, S.Y. Zhang, Z.W. Dai, Mater. Res. Bull. **47**, 212–216 (2012)
6. M. Maczka, A. Bednarkiewicz, E.M. Mendoza, A.F. Fuentes, L. Kepinski, J. Solid State Chem. **194**, 264–269 (2012)
7. S. Chemingui, M. Ferhi, K. Horchani-Naifer, M. Ferid, J. Lumin. **166**, 82–87 (2015)
8. J. Kaur, D. Singh, N.S. Suryanarayana, V. Dubey, J. Display Technol. **12**(9), 928–932 (2016)
9. P.Z. Zambare, K.D. Girase, K.V.R. Murthy, O.H. Mahajan, Adv. Mat. Lett. **4**, 577 (2013)
10. B. Mar, K.C. Singh, M. Sahal, S.P. Khatkar, V.B. Taxak, M. Kumar, J. Lumin. **130**, 2128 (2010)
11. P.Z. Zambare, K.D. Girase, K.V.R. Murthy, O.H. Mahajan, Adv. Mat. Lett. **4**, 577 (2013)
12. J. Kaur, D. Singh, V. Dubey, N.S. Suryanarayana, Y. Parganiha, P. Jha, Res. Chem. Intermed. **40**(8), 2737–2771 (2014)
13. H.M. Rietveld, J. Appl. Cryst. **2**, 65–71 (1969)
14. Z. Qi, C. Shi, G. Zhang, Z. Han, H.H. Hung, Phys. Stat. Sol. (a) **195**(2), 311–316 (2013)
15. V.K. Mathur, A.C. Lewandowski, N.A. Guardala, J.L. Price, Radiat. Measur. **30**, 735 (1999)
16. C. Furetta, *Handbook of Thermoluminescence* (World Scientific, Singapore, 2003)
17. R. Chen, Y. Krish, *Analysis of thermally stimulated process* (Pergamon Press, Oxford, 1981)

18. R. Chen, S.W.S. Mckeever, *Theory of Thermoluminescence and Related Phenomenon* (World Scientific, Singapore, 1997)
19. Springer Handboook of Lasers and Optics, edited by Frank Trager (2012)
20. G.H. Dieke, S. Singh, J. Opt. Soc. Am. **46**, 495 (1956)
21. K. Lemanski, P.J. Deren, J. Rare Earths **29**(12), 1195 (2011)
22. G. Li, J. Guoqi, Y. Baozhu, L. Xu, J. Litao, Y. Zhiping, F. Guangsheng, J. Rare Earth **29**, 540 (2011)
23. K.N. Shinde, S.J. Dhoble, A. Kumar, J. Lumin. **131**, 931 (2011)
24. M. Jayasimhadri, K. Jang, H.S. Lee, B. Chen, S.S. Yi, J.H. Joeng, J. Appl. Phys. **106**, 013105 (2009)